Universal and Updatable Artificial Intelligence-Enhanced Quantum Chemical Foundational Models

Yuxinxin Chen,[1] Yi-Fan Hou,[1] Olexandr Isayev,[2] Pavlo O. Dral[1,3*]

[1]*State Key Laboratory of Physical Chemistry of Solid Surfaces, Fujian Provincial Key Laboratory of Theoretical and Computational Chemistry, Department of Chemistry, and College of Chemistry and Chemical Engineering, Xiamen University, Xiamen 361005, China.*

[2]*Department of Chemistry, Carnegie Mellon University, Pittsburgh, Pennsylvania 15213, United States.*

[3]*Institute of Physics, Faculty of Physics, Astronomy, and Informatics, Nicolaus Copernicus University in Toruń, ul. Grudziądzka 5, 87-100 Toruń, Poland.*

Email: dral@xmu.edu.cn

Abstract

Quantum chemical methods developed since 1927 are instrumental in chemical simulations but human expertise has been still essential in choosing a suitable method. Here we introduce a paradigm shift to universal and updatable artificial intelligence-enhanced quantum mechanical (UAIQM) foundational models with an online platform auto-selecting the models with the best accuracy for the given system, available time, and moderate computational resources (see https://xacs.xmu.edu.cn/docs/mlatom/tutorial_uaiqm.html for instructions). The platform hosts a growing library of state-of-the-art UAIQM models with calibrated uncertainties and provides a mechanism for improving the foundational models continuously with more usage. We demonstrate how the UAIQM platform can be used for massive accurate simulations within hours on a commodity hardware which would take days or weeks on high-performance computing centers with less accurate workhorse quantum chemical methods. We also show that UAIQM sets a new standard for infrared spectra, reaction barriers, and energetics whose accurate predictions can have far-reaching consequences in molecular simulations.

Nearly a century ago, in 1927, the first quantum chemical calculations on the hydrogen atom were performed.[1] Since then, quantum chemical simulations have firmly entranced in fundamental and applied science and engineering, where they help deepen our understanding of physicochemical phenomena and design new materials and drugs. The usefulness of these simulations depends on the accuracy which is severely limited by the computational cost of the quantum mechanical (QM) treatment. Hence, many QM methods have been developed to balance the opposing requirements for accuracy and cost and human expertise has been needed to choose a suitable method (Figure 1a).

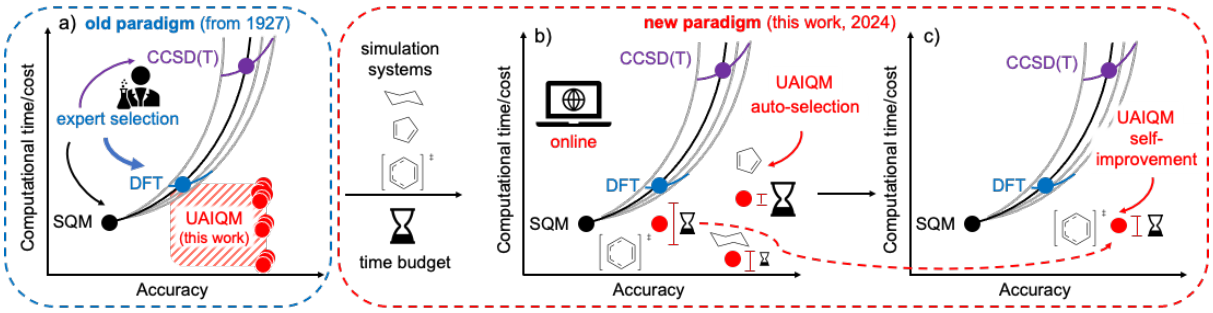

Figure 1. Paradigm shift in computational chemistry introduced in this work with the UAIQM platform. a) In the old paradigm, the specific QM methods have been chosen manually based on considerations of optimal cost/accuracy tradeoff. b) In the new paradigm, the online platform chooses an optimal UAIQM method for a given time budget for each specific system based on the calibrated uncertainty quantification. c) The platform can self-improve when encountering problematic systems with high uncertainty. UAIQM platform currently contains a dozen methods of varying speed (from fast universal neural network potentials to AI-enhanced semi-empirical QM and DFT methods) targeting gold-standard CCSD(T)/CBS accuracy.

In a quest to improve the accuracy and speed of QM methods, artificial intelligence (AI) models have emerged to the point that they can be used instead of QM methods in simulations, e.g., in molecular dynamics (MD) where AI models are used as surrogate models.[2-14] Another big class of methods uses AI to improve the accuracy of the baseline QM methods resulting in more transferable and robust hybrid approaches.[14-18] While many approaches are proof-of-concept, AI-based methods for out-of-the-box use in general-purpose atomistic simulations are rapidly proliferating. Universal neural network (NN) potentials such as those of ANI,[19] AIMnet,[20] MACE,[21] and DPA[22] families offer faster alternatives to the QM methods for a broad class of compounds and conformers while maintaining good accuracy approaching the QM level they were trained on. Methods such as DM21,[23] CF22D,[24] and DeePKS[25] use NNs to improve density functional theory (DFT) approaches and AIQM1,[26] OrbNet Denali,[27] and QDπ[28] improve upon low-cost semi-empirical QM treatment, usually to a DFT level. Our original AIQM1 method has excellent accuracy approaching gold-standard coupled cluster

singles, doubles, and perturbative triples method with complete basis set extrapolation (CCSD(T)/CBS), while maintaining the high speed of semi-empirical QM methods for many properties and is applicable for rather big systems.

Despite all the apparent success, the realization is growing that any method has and, in the foreseeable future, will have unsatisfactory performance for some simulations. To give several examples, DeepMind's DM21 was later found to have problems with water simulations[29] and transition metal complexes[30]. Our AIQM1 was found to have lower accuracy for the properties its NNs were not trained on, e.g., for reaction barriers.[31] NN models such as ANI-1ccx[32] can have sub-par accuracy for large conjugated systems.[26]

With the realization that no single model can fit all needs, here, we put forward a paradigm shift in atomistic simulations from focusing on a single AI or QM method to using a platform offering the best solution for a given problem and given resources (time budget and computing hardware) (Figure 1b). For this, we introduce a unified platform for computational chemistry, implemented based on MLatom[33] and available online,[34] that provides universal and updatable AI-enhanced QM (UAIQM) foundational models (see instructions at https://xacs.xmu.edu.cn/docs/mlatom/tutorial_uaiqm.html). This platform is continuously improved with more data and a growing number of models with increasing accuracy and transferability (Figure 1c). At the moment of writing, we have a dozen models ranging from universal NN potentials to NN-improved QM baselines of different levels (from semi-empirical QM to hybrid Kohn–Sham DFT with double- and triple-ζ basis sets) (see SI note 1, Supplementary Information, SI). AIQM1 and ANI-1ccx are part of this library. With the understanding that the platform is under continuous improvement, here we describe the platform's capabilities at the moment of writing (June 2024).

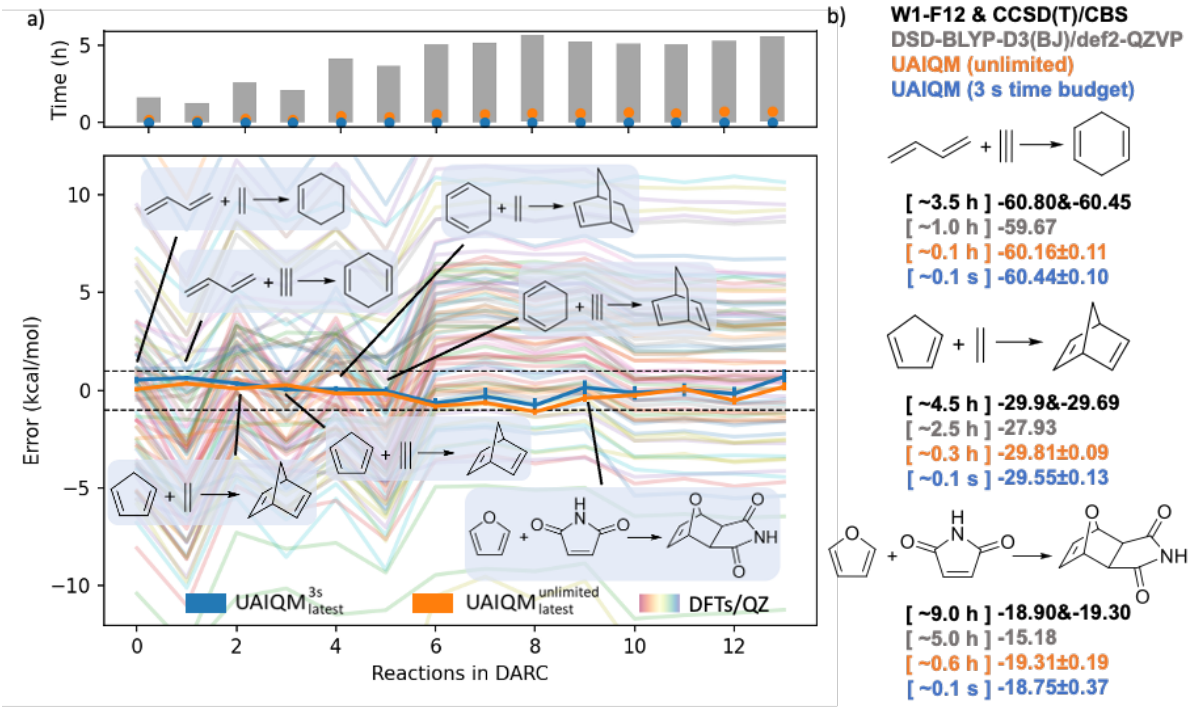

Figure 2. Performance of auto-selected UAIQM and 84 functionals, benchmarked in previously,[35] on the Diels–Alder reactions (DARC)[35, 36]. a) Error of reaction energy and calculation time for each reaction. b) Comparison of time and reaction energies on representative reactions with W1-F12 & CCSD(T)/CBS (black, time for CCSD(T)/CBS), DSD-BLYP-D3(BJ)/def2-QZVP (grey), UAIQM at time budget 3s (blue) and at unlimited time budget (orange). Energies are in kcal/mol, the calculation time – CPU-hour.

One of the key UAIQM platform's features is our robust auto-selection procedure that finds the most suitable method for the given system and time budget Figure 1b). The auto-selection is based on the cost of the QM baseline and the calibrated uncertainty quantification (UQ) (see SI note 2). We extend our previously developed[37] scheme for calibrating UQ of the foundational AIQM1 and ANI-1ccx models. This UQ provides important additional information that standard QM methods do not give. For systems with low UQ metrics, the UAIQM typically provides simulations with chemical accuracy (errors below 1 kcal/mol compared to the reference high-level reaction energies). Examples are shown in Figure 2 for the Diels–Alder reactions. Even with the time budget of 3 s per simulation, we can easily reach chemical accuracy with confidence (low UQ metrics), while some of the best DFT functionals such as slow double-hybrid density functional DSD-BLYP-D3(BJ) taking hours to calculate fail to be as accurate (Figure 2b). In general, DFT methods have a very broad spread in errors (Figure 2a), and, without extra expert intervention and additional higher-level slow QM

computations, it has been impossible to guarantee chemically accurate reaction energies before the UAIQM introduction.

Many simulations such as molecular dynamics may have even stricter time-budget limitations. One example is the recourse-intensive downhill molecular dynamics (MD) simulations of a pericyclic reaction starting from the region around the ambimodal transition states (TS, Figure 3a). Here, we can reduce the time budget to as little as 0.1 s per time step to enable extensive explorations on commodity hardware within half a day with 1000 quasi-classical MD trajectories, each 500 fs long with 1 fs time step (in total half a million single-point evaluations, see SI note 3 for computational details). This dynamics on a smaller scale (only 117 reactive trajectories) was performed earlier with a much costlier DFT method B3LYP-D3/6-31G* chosen by human experts,[38] which would take 16 CPU-years for a thousand trajectories on the same hardware. Our auto-selection scheme has chosen AIQM2 and the detailed results obtained with AIQM2 for this reaction are described in the dedicated work[39]. In brief, method AIQM2 revised the DFT calculations[38] to show that a much smaller fraction (3% rather than 9%) of reactive trajectories leads to a minor product **P1** (Figure 3a).

Another example is accurate infrared (IR) spectra including anharmonic and quantum nuclear effects.[40] Such spectrum simulations require extensive computations with, e.g., path-integral MD and can be readily performed with the fastest UAIQM methods, e.g., AIQM1. The resulting IR spectra are obtained within 1.5 CPU-h while having the coupled-cluster accuracy and closely resembling the experimental spectra as shown in an example of ethanol in the gas phase (Figure 3b, SI note 4).

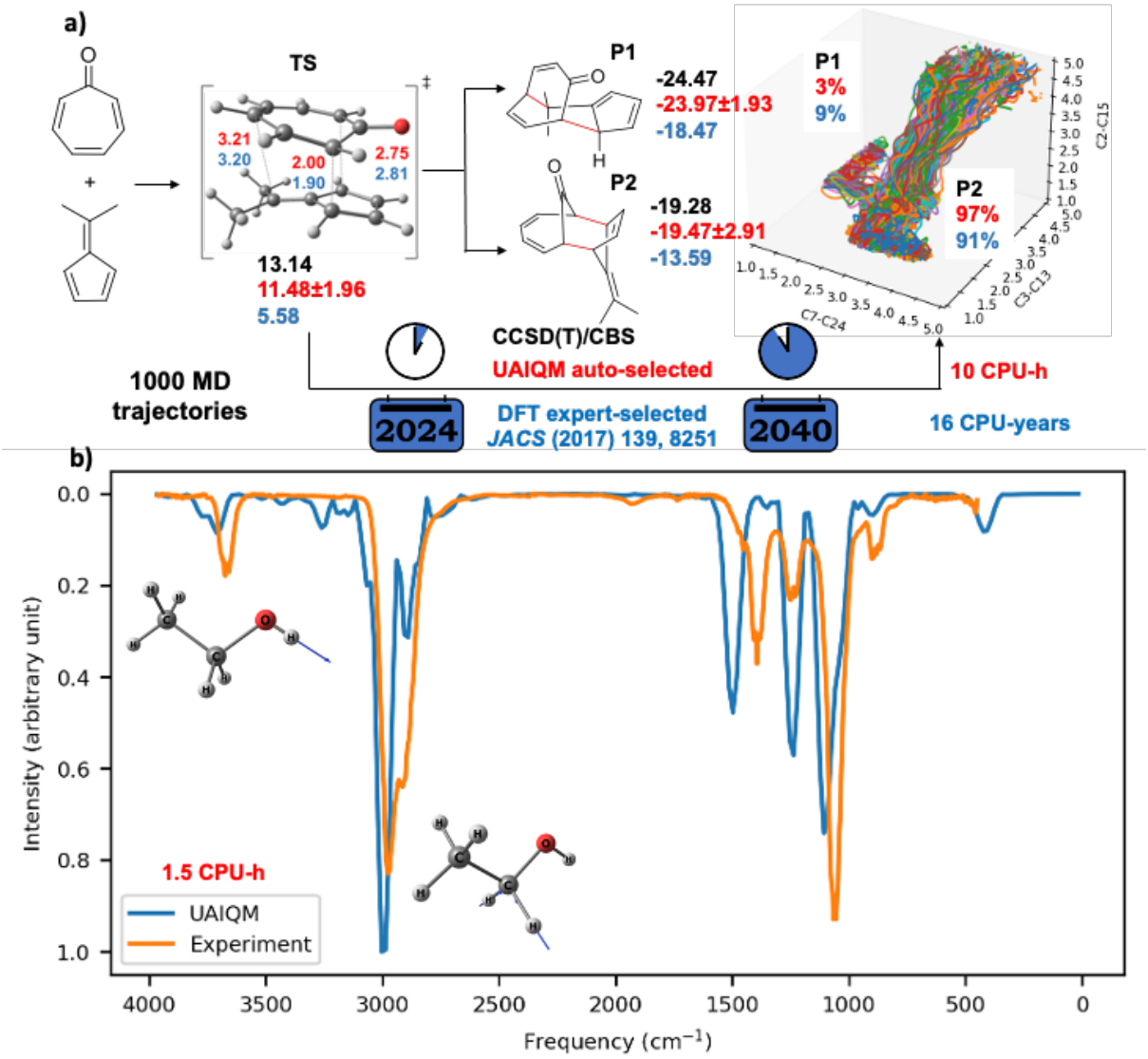

Figure 3. Low time-budget extensive simulations with UAIQM methods. a) Quasiclassical trajectories analysis on the bifurcating pericyclic reaction between tropone and dimethylfulvene, adapted from the dedicated study[38] on AIQM2 (which was auto-selected by UAIQM). Reaction energies in black are derived from CCSD(T)/CBS single-point calculations on the B3LYP-D3/6-31G*-optimized geometry. The unit for bond length is Ångstrom and energy – kcal/mol. b) Infrared spectrum of ethanol from path integral molecular dynamics with AIQM1 belonging to the UAIQM library compared to the experimental spectrum[41].

Inevitably, in some cases, the uncertainty and errors are much higher than our current target of CCSD(T)/CBS. Hence, we developed a procedure to improve the models by generating additional data for such systems and refining models. Let's take the pericyclic reactions for which the fast UAIQM methods had unsatisfactory accuracy with high uncertainty (the slower methods were within chemical accuracy). Our improving procedure produced a new generation of UAIQM models which now reach chemical accuracy for such reactions (Figure 4).

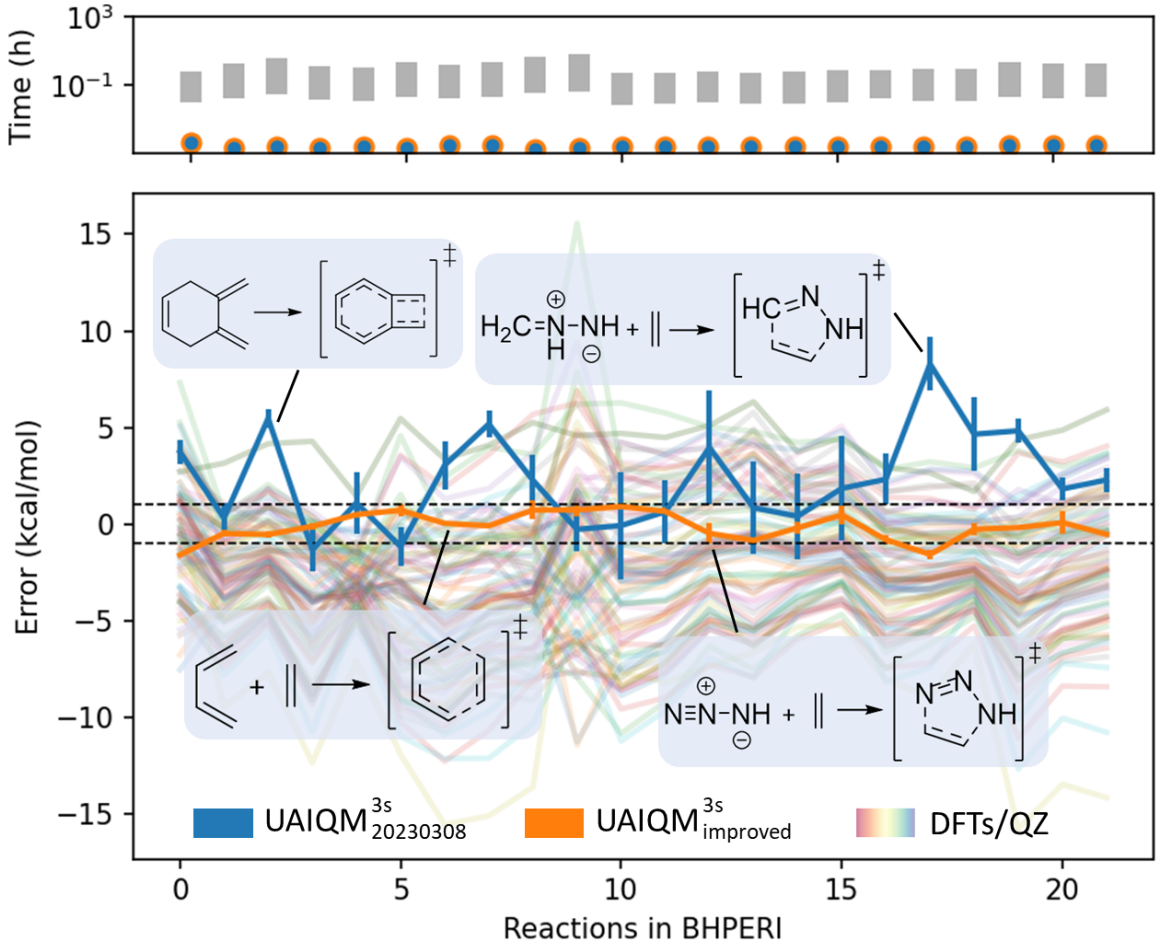

Figure 4. Performance of the original and improved UAIQM methods and 84 functionals, benchmarked previously[35], on the BHPERI data set[35, 42-44]. The results in orange correspond to the UAIQM method at time-budget 3 s that was allowed to improve on the BHPERI dataset. Time is estimated on 16 CPUs.

The above results were limited to the neutral, closed-shell compounds with the CHNO elements due to the availability of the accurate coupled-cluster level data (see SI note 5). However, many of our models are available for molecular and supermolecular systems with elements across the periodic table (see SI note 1). Generally, the UAIQM platform ensures the unrivaled, state-of-the-art quality of the simulations for moderate time and hardware resources as is evidenced by the benchmark on the neutral, closed-shell CHNO subset of the standard GMTKN55 set[35] (Figure 5 and SI note 6). The platform also provides good but not excellent quality for other compounds (accuracy similar or better compared to hybrid DFT with a double- and triple-ζ basis sets or semi-empirical QM methods, see SI note 8). At the moment of writing, the models trained on data for seven (CHNOFClS) elements are being generated and will soon

be included in the platform (see the SI note 7 for the preliminary results showing that the semi-empirical baseline model performs similarly to the DFT with triple-ζ basis set).

*real time tested on 16 CPUs		UAIQM				B3LYP-D4/	DSD-BLYP-D4/	DSD-BLYP-D3(BJ)/	DM21/		CCSD(T)*/
		0th generation	0th generation	2024.03.08	2024.03.08						
	Time budget	3s	Infinite	3s	Infinite	6-31G*	6-31G*	def2-QZVP	6-31G*	def2-QZVP	CBS
	Time used*	~0.03 h	~100 h	~0.03 h	~200 h	~10 h	~15 h	~900 h	~70 h	~1400 h	~1500 h
Subsets	**N**	**basic properties and reaction energies for small systems**									
G2RC	12	7.87	7.40	1.38	1.28	10.66	9.56	1.34	8.84	1.25	0.89
FH51	44	2.38	2.43	0.79	0.46	5.75	3.97	1.16	5.07	1.02	0.34
TAUT15	13	0.34	0.29	0.42	0.30	1.59	1.99	0.47	1.76	0.45	0.20
DC13	10	7.70	4.92	3.72	2.47	5.99	4.58	3.34	7.02	3.45	1.49
WTMAD-2		2.59	2.32	1.21	0.82	5.50	5.00	1.39	5.33	1.31	0.47
		reaction energies for large systems and isomerisation reactions									
DARC	13	0.37	0.37	0.31	0.39	2.08	6.01	2.39	2.75	1.06	0.30
BSR36	36	0.32	0.37	0.52	0.38	3.14	0.74	1.49	7.97	0.51	0.19
CDIE20	20	0.76	0.53	0.89	0.29	1.95	1.30	0.56	1.14	0.35	0.19
ISO34	34	0.38	0.37	0.29	0.26	2.89	2.35	0.69	2.69	0.58	0.21
ISOL24	16	1.82	0.90	1.34	0.71	3.65	2.77	2.49	4.71	1.30	0.21
C60ISO	9	2.74	14.80	26.85	15.33	2.55	6.78	7.63	11.74	11.35	-
WTMAD-2		1.24	1.17	1.74	0.88	4.83	3.32	1.97	6.27	1.18	0.36
		reaction barrier heights									
BHPERI	22	2.54	1.20	2.96	1.09	4.02	4.07	1.77	1.97	0.85	0.26
BHDIV10	5	6.97	3.20	1.25	1.56	4.22	4.21	1.81	2.70	2.11	0.21
INV24	13	1.17	0.77	1.42	0.78	1.68	1.27	0.66	2.22	0.97	0.28
BHROT27	19	0.34	0.16	0.27	0.15	0.75	0.66	0.22	0.51	0.19	0.12
PX13	8	5.74	1.36	1.05	1.25	8.34	2.59	1.46	3.68	1.07	0.33
WCPT18	12	1.69	1.32	1.31	1.53	6.49	4.17	1.08	4.43	1.61	0.19
WTMAD-2		2.03	0.97	1.67	0.89	3.53	2.84	1.14	2.22	0.89	0.26
		intermolecular noncovalent interactions									
ADIM6	6	1.54	0.87	0.35	0.74	0.47	0.12	0.37	4.35	0.11	0.04
S22	22	1.08	0.51	0.94	0.26	2.58	2.07	0.17	2.63	0.20	0.13
S66	66	0.66	0.35	0.58	0.32	2.10	1.63	0.17	2.30	0.18	0.09
WATER27	15	1.56	0.80	1.11	1.06	55.36	46.70	1.11	41.69	2.46	0.70
WTMAD-2		3.03	1.60	2.27	1.31	9.34	7.36	0.73	10.70	0.73	0.30
		intramolecular noncovalent interactions									
IDISP	6	3.81	0.06	1.01	1.28	1.82	2.52	1.02	9.86	1.37	-
ACONF	15	0.27	0.17	0.24	0.16	0.19	0.10	0.19	0.72	0.13	0.03
Amino20x4	72	0.49	0.39	0.39	0.17	0.71	0.61	0.14	0.58	0.19	0.11
PCONF21	18	0.45	0.38	0.71	0.26	1.88	1.83	0.23	1.48	0.27	0.37
MCONF	51	0.47	0.20	0.45	0.35	1.37	1.12	0.30	1.56	0.22	1.71
SCONF	17	0.71	0.12	0.85	0.17	3.66	3.41	0.06	2.93	0.36	0.06
BUT14DIOL	64	0.36	0.07	0.29	0.10	2.44	2.02	0.06	1.72	0.17	0.14
WTMAD-2		3.69	1.69	3.42	1.53	12.15	10.53	1.28	10.41	1.67	1.10
Total WTMAD-2		2.74	1.56	2.40	1.19	8.31	6.89	1.32	7.98	1.27	0.63

Figure 5. Performance assessment of the UAIQM platform compared to a selection of the QM and AI-enhanced QM methods on the GMTKN55 data set[35]. Results are shown for the neutral closed-shell CHNO-containing compounds based on the auto-selection of UAIQM methods (results for different UAIQM methods are given in SI note 6 and for full GMTKN55 in SI note 8). Time is estimated on 16 CPUs. Numbers are mean absolute errors in kcal/mol. WTMAD-2 – weighted mean absolute deviation-2 in kcal/mol as defined in Ref. [35]. MAE of two subsets are missing in CCSD(T)*/CBS results due to unaffordable time cost.

The overall error for the fast UAIQM models (with certain and uncertain predictions) is much smaller than of a typical Kohn–Sham hybrid DFT functional with a double-ζ quality (0.03 vs ~10 CPU-hours for the benchmark on the neutral, closed-shell, CHNO-containing compounds, Figure 5). This is true for both 0th iteration of UAIQM which knew nothing about GMTKN55 and for later iterations of UAIQM which we allowed to improve on a limited number (six) of GMTKN55 subsets it was performing badly (see SI note 5). The best UAIQM solutions are slower (~200 CPU-hours) but also have errors smaller than much more

computationally expensive double-hybrid DFT functional or ML-improved DM21 with the quadruple-ζ basis set (~1000-CPU hours). Considering that GMTKN55 only needs single-point calculations on relatively small molecules, such slow QM and ML-improved QM methods would be infeasible for, e.g., geometry optimizations, dynamics, and thermochemical property calculations of bigger systems.

UAIQM provides a totally practical solution and can easily perform various types of simulations with high accuracy. While above we showed its prowess for energy calculations, dynamics, and IR spectra simulations, the methods should be applicable in other simulations, e.g., for emission spectra[45] and excited-state dynamics[46] as was shown for the platform's predecessor AIQM1 which is part of the library of UAIQM models. The final remark is that the online availability of the UAIQM platform is enabling calculations around the world for research groups with varying access to computational resources. This contributes to the important goal of democratization of high-quality QM simulations which previously have only been available to the groups with access to more hardware resources.

Author contributions

P.O.D.: conceptualization, method design, original draft, figures. Y.C.: method development and implementations, calculations, analysis, manuscript revision, figures. O.I.: discussion of method training and databases, supply of databases, manuscript and figures revision. Y.F.Hou: implementation and analysis of PIMD calculations.

Acknowledgments

P.O.D. acknowledges funding by the National Natural Science Foundation of China (No. 22003051 and funding via the Outstanding Youth Scholars (Overseas, 2021) project), the Fundamental Research Funds for the Central Universities (No. 20720210092), and via the Lab project of the State Key Laboratory of Physical Chemistry of Solid Surfaces. Y.C. thanks Peikun Zheng for his help with training models at the beginning of the project.

References

1. Heitler, W.; London, F., Wechselwirkung neutraler Atome und homöopolare Bindung nach der Quantenmechanik. *Z. Phys.* **1927,** *44*, 455–472.

2. Aldossary, A.; Campos‐Gonzalez‐Angulo, J. A.; Pablo‐García, S.; Leong, S. X.; Rajaonson, E. M.; Thiede, L.; Tom, G.; Wang, A.; Avagliano, D.; Aspuru‐Guzik, A., In Silico Chemical Experiments in the Age of AI: From Quantum Chemistry to Machine Learning and Back. *Adv. Mater.* **2024,** *Early View*, 2402369.

3. Zhang, J.; Chen, D.; Xia, Y.; Huang, Y. P.; Lin, X.; Han, X.; Ni, N.; Wang, Z.; Yu, F.; Yang, L.; Yang, Y. I.; Gao, Y. Q., Artificial Intelligence Enhanced Molecular Simulations. *J. Chem. Theory Comput.* **2023,** *19*, 4338-4350.

4. Huang, B.; von Rudorff, G. F.; von Lilienfeld, O. A., The central role of density functional theory in the AI age. *Science* **2023,** *381*, 170–175.

5. Hermann, J.; Spencer, J.; Choo, K.; Mezzacapo, A.; Foulkes, W. M. C.; Pfau, D.; Carleo, G.; Noé, F., Ab initio quantum chemistry with neural-network wavefunctions. *Nat. Rev. Chem.* **2023,** *7*, 692–709.

6. Kulik, H. J.; Hammerschmidt, T.; Schmidt, J.; Botti, S.; Marques, M. A. L.; Boley, M.; Scheffler, M.; Todorović, M.; Rinke, P.; Oses, C.; Smolyanyuk, A.; Curtarolo, S.; Tkatchenko, A.; Bartók, A. P.; Manzhos, S.; Ihara, M.; Carrington, T.; Behler, J.; Isayev, O.; Veit, M.; Grisafi, A.; Nigam, J.; Ceriotti, M.; Schütt, K. T.; Westermayr, J.; Gastegger, M.; Maurer, R. J.; Kalita, B.; Burke, K.; Nagai, R.; Akashi, R.; Sugino, O.; Hermann, J.; Noé, F.; Pilati, S.; Draxl, C.; Kuban, M.; Rigamonti, S.; Scheidgen, M.; Esters, M.; Hicks, D.; Toher, C.; Balachandran, P. V.; Tamblyn, I.; Whitelam, S.; Bellinger, C.; Ghiringhelli, L. M., Roadmap on Machine learning in electronic structure. *Electron. Struct.* **2022,** *4*, 023004.

7. Deringer, V. L.; Bartok, A. P.; Bernstein, N.; Wilkins, D. M.; Ceriotti, M.; Csanyi, G., Gaussian Process Regression for Materials and Molecules. *Chem. Rev.* **2021,** *121*, 10073–10141.

8. von Lilienfeld, O. A.; Müller, K.-R.; Tkatchenko, A., Exploring chemical compound space with quantum-based machine learning. *Nat. Rev. Chem.* **2020,** *4*, 347–358.

9. Butler, K. T.; Davies, D. W.; Cartwright, H.; Isayev, O.; Walsh, A., Machine learning for molecular and materials science. *Nature* **2018,** *559*, 547–555.

10. Unke, O. T.; Chmiela, S.; Sauceda, H. E.; Gastegger, M.; Poltavsky, I.; Schutt, K. T.; Tkatchenko, A.; Muller, K. R., Machine Learning Force Fields. *Chem. Rev.* **2021,** *121*, 10142–10186.

11. Musil, F.; Grisafi, A.; Bartók, A. P.; Ortner, C.; Csányi, G.; Ceriotti, M., Physics-inspired structural representations for molecules and materials. *Chem. Rev.* **2021,** *121*, 9759–9815.

12. Behler, J., Four Generations of High-Dimensional Neural Network Potentials. *Chem. Rev.* **2021,** *121*, 10037–10072.

13. Bowman, J. M.; Qu, C.; Conte, R.; Nandi, A.; Houston, P. L.; Yu, Q., Delta-Machine Learned Potential Energy Surfaces and Force Fields. *J. Chem. Theory Comput.* **2023,** *19*, 1–17.

14. Dral, P. O., *Quantum Chemistry in the Age of Machine Learning*. Elsevier: Amsterdam, Netherlands, 2023.

15. Ramakrishnan, R.; Dral, P. O.; Rupp, M.; von Lilienfeld, O. A., Big Data Meets Quantum Chemistry Approximations: The Δ-Machine Learning Approach. *J. Chem. Theory Comput.* **2015,** *11*, 2087–2096.

16. Fedik, N.; Nebgen, B.; Lubbers, N.; Barros, K.; Kulichenko, M.; Li, Y. W.; Zubatyuk, R.; Messerly, R.; Isayev, O.; Tretiak, S., Synergy of semiempirical models and machine learning in computational chemistry. *J. Chem. Phys.* **2023,** *159*, 110901.

17. Westermayr, J.; Gastegger, M.; Schütt, K. T.; Maurer, R. J., Perspective on integrating machine learning into computational chemistry and materials science. *J. Chem. Phys.* **2021,** *154*, 230903.

18. Qiao, Z.; Christensen, A. S.; Welborn, M.; Manby, F. R.; Anandkumar, A.; Miller, T. F., Informing geometric deep learning with electronic interactions to accelerate quantum chemistry. *Proc. Natl. Acad. Sci. U.S.A.* **2022,** *119*, e2205221119.

19. Gao, X.; Ramezanghorbani, F.; Isayev, O.; Smith, J. S.; Roitberg, A. E., TorchANI: A Free and Open Source PyTorch-Based Deep Learning Implementation of the ANI Neural Network Potentials. *J. Chem. Inf. Model.* **2020,** *60*, 3408–3415.

20. Zubatyuk, R.; Smith, J. S.; Leszczynski, J.; Isayev, O., Accurate and transferable multitask prediction of chemical properties with an atoms-in-molecules neural network. *Sci. Adv.* **2019,** *5*, eaav6490.

21. Batatia, I.; Benner, P.; Chiang, Y.; Elena, A. M.; Kovács, D. P.; Riebesell, J.; Advincula, X. R.; Asta, M.; Avaylon, M.; Baldwin, W. J.; Berger, F.; Bernstein, N.; Bhowmik, A.; Blau, S. M.; Cărare, V.; Darby, J. P.; De, S.; Pia, F. D.; Deringer, V. L.; Elijošius, R.; El-Machachi, Z.; Falcioni, F.; Fako, E.; Ferrari, A. C.; Genreith-Schriever, A.; George, J.; Goodall, R. E. A.; Grey, C. P.; Grigorev, P.; Han, S.; Handley, W.; Heenen, H. H.; Hermansson, K.; Holm, C.; Jaafar, J.; Hofmann, S.; Jakob, K. S.; Jung, H.; Kapil, V.; Kaplan, A. D.; Karimitari, N.; Kermode, J. R.; Kroupa, N.; Kullgren, J.; Kuner, M. C.; Kuryla, D.; Liepuoniute, G.; Margraf, J. T.; Magdău, I.-B.; Michaelides, A.; Moore, J. H.; Naik, A. A.; Niblett, S. P.; Norwood, S. W.; O'Neill, N.; Ortner, C.; Persson, K. A.; Reuter, K.; Rosen, A. S.; Schaaf, L. L.; Schran, C.; Shi, B. X.; Sivonxay, E.; Stenczel, T. K.; Svahn, V.; Sutton, C.; Swinburne, T. D.; Tilly, J.; Oord, C. v. d.; Varga-Umbrich, E.; Vegge, T.; Vondrák, M.; Wang, Y.; Witt, W. C.; Zills, F.; Csányi, G., A foundation model for atomistic materials chemistry. *arXiv:2401.00096v2 [physics.chem-ph]* **2024**.

22. Zhang, D.; Bi, H.; Dai, F.-Z.; Jiang, W.; Liu, X.; Zhang, L.; Wang, H., Pretraining of attention-based deep learning potential model for molecular simulation. *npj Computational Materials* **2024,** *10*, 94.

23. Kirkpatrick, J.; McMorrow, B.; Turban, D. H. P.; Gaunt, A. L.; Spencer, J. S.; Matthews, A.; Obika, A.; Thiry, L.; Fortunato, M.; Pfau, D.; Castellanos, L. R.; Petersen, S.; Nelson, A. W. R.; Kohli, P.; Mori-Sanchez, P.; Hassabis, D.; Cohen, A. J., Pushing the frontiers of density functionals by solving the fractional electron problem. *Science* **2021,** *374*, 1385–1389.

24. Liu, Y.; Zhang, C.; Liu, Z.; Truhlar, D. G.; Wang, Y.; He, X., Supervised learning of a chemistry functional with damped dispersion. *Nat. Comput. Sci.* **2022,** *3*, 48–58.

25. Chen, Y.; Zhang, L.; Wang, H.; E, W., DeePKS: A Comprehensive Data-Driven Approach toward Chemically Accurate Density Functional Theory. *J. Chem. Theory Comput.* **2020**.

26. Zheng, P.; Zubatyuk, R.; Wu, W.; Isayev, O.; Dral, P. O., Artificial Intelligence-Enhanced Quantum Chemical Method with Broad Applicability. *Nat. Commun.* **2021,** *12*, 7022.

27. Christensen, A. S.; Sirumalla, S. K.; Qiao, Z.; O'Connor, M. B.; Smith, D. G. A.; Ding, F.; Bygrave, P. J.; Anandkumar, A.; Welborn, M.; Manby, F. R.; Miller, T. F., 3rd, OrbNet Denali: A machine learning potential for biological and organic chemistry with semi-empirical cost and DFT accuracy. *J. Chem. Phys.* **2021,** *155*, 204103.

28. Zeng, J.; Tao, Y.; Giese, T. J.; York, D. M., QDπ: A Quantum Deep Potential Interaction Model for Drug Discovery. *J. Chem. Theory Comput.* **2023,** *19*, 1261–1275.

29. Palos, E.; Lambros, E.; Dasgupta, S.; Paesani, F., Density functional theory of water with the machine-learned DM21 functional. *J. Chem. Phys.* **2022,** *156*, 161103.

30. Zhao, H.; Gould, T.; Vuckovic, S., Deep Mind 21 functional does not extrapolate to transition metal chemistry. *Physical Chemistry Chemical Physics* **2024,** *26*, 12289-12298.

31. Chen, Y.; Ou, Y.; Zheng, P.; Huang, Y.; Ge, F.; Dral, P. O., Benchmark of General-Purpose Machine Learning-Based Quantum Mechanical Method AIQM1 on Reaction Barrier Heights. *J. Chem. Phys.* **2023,** *158*, 074103.

32. Smith, J. S.; Nebgen, B. T.; Zubatyuk, R.; Lubbers, N.; Devereux, C.; Barros, K.; Tretiak, S.; Isayev, O.; Roitberg, A. E., Approaching coupled cluster accuracy with a general-purpose neural network potential through transfer learning. *Nat. Commun.* **2019,** *10*, 2903.

33. Dral, P. O.; Ge, F.; Hou, Y.-F.; Zheng, P.; Chen, Y.; Barbatti, M.; Isayev, O.; Wang, C.; Xue, B.-X.; Pinheiro Jr, M.; Su, Y.; Dai, Y.; Chen, Y.; Zhang, S.; Zhang, L.; Ullah, A.; Zhang, Q.; Ou, Y., MLatom 3: A Platform for Machine Learning-Enhanced Computational Chemistry Simulations and Workflows. *J. Chem. Theory Comput.* **2024,** *20*, 1193–1213.

34. The computations can be performed on the XACS cloud computing platform at https://XACScloud.com.

35. Goerigk, L.; Hansen, A.; Bauer, C.; Ehrlich, S.; Najibi, A.; Grimme, S., A look at the density functional theory zoo with the advanced GMTKN55 database for general main group thermochemistry, kinetics and noncovalent interactions. *Phys. Chem. Chem. Phys.* **2017,** *19*, 32184–32215.

36. Johnson, E. R.; Mori-Sánchez, P.; Cohen, A. J.; Yang, W., Delocalization errors in density functionals and implications for main-group thermochemistry. *J. Chem. Phys.* **2008,** *129*, 204112.

37. Zheng, P.; Yang, W.; Wu, W.; Isayev, O.; Dral, P. O., Toward Chemical Accuracy in Predicting Enthalpies of Formation with General-Purpose Data-Driven Methods. *J. Phys. Chem. Lett.* **2022,** *13*, 3479–3491.

38. Yu, P.; Chen, T. Q.; Yang, Z.; He, C. Q.; Patel, A.; Lam, Y. H.; Liu, C. Y.; Houk, K. N., Mechanisms and Origins of Periselectivity of the Ambimodal [6 + 4] Cycloadditions of Tropone to Dimethylfulvene. *J. Am. Chem. Soc.* **2017,** *139*, 8251–8258.

39. Chen, Y.; Dral, P. O., AIQM2: Better Reaction Simulations with the 2nd Generation of General-Purpose AI-enhanced Quantum Mechanical Method. *ChemRxiv* **2024**.

40. Xu, X.; Chen, Z.; Yang, Y., Molecular Dynamics with Constrained Nuclear Electronic Orbital Density Functional Theory: Accurate Vibrational Spectra from Efficient Incorporation of Nuclear Quantum Effects. *J. Am. Chem. Soc.* **2022,** *144*, 4039–4046.

41. Linstrom, E. P.; Mallard, W., NIST Chemistry WebBook, NIST Standard Reference Database Number 69. https://webbook.nist.gov/chemistry/.

42. Guner, V.; Khuong, K. S.; Leach, A. G.; Lee, P. S.; Bartberger, M. D.; Houk, K. N., A Standard Set of Pericyclic Reactions of Hydrocarbons for the Benchmarking of Computational Methods: The Performance of ab Initio, Density Functional, CASSCF, CASPT2, and CBS-QB3 Methods for the Prediction of Activation Barriers, Reaction Energetics, and Transition State Geometries. *J. Phys. Chem. A* **2003,** *107*, 11445–11459.

43. Dinadayalane, T. C.; Vijaya, R.; Smitha, A.; Sastry, G. N., Diels−Alder Reactivity of Butadiene and Cyclic Five-Membered Dienes ($(CH)_4X$, X = CH_2, SiH_2, O, NH, PH, and S) with Ethylene: A Benchmark Study. *J. Phys. Chem. A* **2002,** *106*, 1627–1633.

44. Ess, D. H.; Houk, K. N., Activation Energies of Pericyclic Reactions: Performance of DFT, MP2, and CBS-QB3 Methods for the Prediction of Activation Barriers and Reaction Energetics of 1,3-Dipolar Cycloadditions, and Revised Activation Enthalpies for a Standard Set of Hydrocarbon Pericyclic Reactions. *J. Phys. Chem. A* **2005,** *109*, 9542–9553.

45. Schaub, T. A.; Zieleniewska, A.; Kaur, R.; Minameyer, M.; Yang, W.; Schüßlbauer, C. M.; Zhang, L.; Freiberger, M.; Zakharov, L. N.; Drewello, T.; Dral, P. O.; Guldi, D.; Jasti, R., Tunable Macrocyclic Polyparaphenylene Nanolassos via Copper‐Free Click Chemistry. *Chem. Eur. J.* **2023,** *29*, e202300668.

46. Zhang, L.; Pios, S. V.; Martyka, M.; Ge, F.; Hou, Y. F.; Chen, Y.; Chen, L.; Jankowska, J.; Barbatti, M.; Dral, P. O., MLatom Software Ecosystem for Surface Hopping Dynamics in Python with Quantum Mechanical and Machine Learning Methods. *J. Chem. Theory Comput.* **2024,** *20*, 5043–5057.